Photo-Conductance from Exciton Binding in Molecular Junctions – Supplementary Information

Jianfeng Zhou [†] , Kun Wang[†], Bingqian Xu[†] and Yonatan Dubi[‡§]

† Single Molecule Study Laboratory, College of Engineering, University of Georgia, Athens, GA 30602, USA.

‡Department of Chemistry, Ben-Gurion University of the Negev, Beer-Sheva 84105 Israel.

[§]Ilse-Katz Institute for Nanoscale Science and Technology, Ben-Gurion University of the Negev, Beer-Sheva 84105 Israel.

1. Model and calculation – Further details

The model for the molecular junction consists of a molecule between two metallic electrodes. We take into account only the HOMO and LUMO molecular levels and spinless Fermions. The corresponding Hamiltonian of the system is

$$\mathcal{H}_0 = \mathcal{H}_M + \mathcal{H}_{L,R-M}$$

$$\mathcal{H}_M = \sum_{n=1}^{2} \epsilon_n d_n^+ d_n + U\hat{n}_1\hat{n}_2$$

$$\mathcal{H}_{L,R-M} = \sum_{k\in\{L,R\}} \epsilon_k c_k^+ c_k + \sum_{k\in\{L,R\}} (V_k c_k^+ d + h.c.) \qquad (1)$$

where c_k (c_k^+) are annihilation (creation) operators for electrons in the electrodes (with energy ϵ_k), d_n (d_n^+) are annihilation (creation) operators for electrons in a molecular level $|n\rangle$ with energy ϵ_n, where $n = 1$ ($n = 2$) marks the HOMO (LUMO) level, $\hat{n}_n = d_n^+ d_n$ is the number operator, and U is the Coulomb term which represents the electrostatic repulsion between electrons in the molecule. Alternatively, $-U$ can be considered as the molecular exciton binding energy, and represents the difference between the optical gap and the fundamental (or transport) gap. We note that in general, when discussing a molecular system with interactions spins should be accounted for, since the spin-degeneracy changes the combinatorics of how an electron can be excited, and consequently may affect the conductance. However, this situation is most important in the absence of particle-hole symmetry. Since in our system both the HOMO and LUMO are far from the Fermi level (many times the ambient temperature), to a very good approximation the particle-hole symmetry is conserved, and therefore accounting for spin only affects the conductance qualitatively (by a multiplicative factor of 2). In any case, even if spins were taken into account in the absence of particle-hole symmetry, the conclusion regarding our suggested mechanism for photoconductivity would remain the same.

Transitions between the HOMO and LUMO are generated by absorption or emission of a photon, represented (in the rotating wave approximation) by the Hamiltonian term

$$\mathcal{H}_1 = \omega_0 a^+ a + \lambda(a^+ d_1^+ d_2 + a d_2^+ d_1) \quad (2)$$

where a (a^+) annihilates (creates) a photon with frequency $\omega_0 = \epsilon_2 - \epsilon_1$ (the resonance condition justifying the rotating wave approximation) and λ is the electron-photon coupling.

In the weak coupling limit (both molecule-electrode and electron-photon), the dynamics of the system can be approximated using the rate (master) equations. Within this approach, the Hamiltonian of the molecular bridge is diagonalized (in Fock space), giving four states, $|\emptyset\rangle, |1,0\rangle, |0,1\rangle, |1,1\rangle$ describing an empty molecule, a molecule with one electron in the HOMO level, a molecule with an excited electron in the LUMO level, and a doubly-occupied molecule. We enumerate by $\mathbf{P} = (P_1, P_2, P_3, P_4)$ the probabilities to find the molecule at each of the above states, with energies $\epsilon_1 = 0, \epsilon_2 = \epsilon_{HOMO}, \epsilon_3 = \epsilon_{LUMO}, \epsilon_4 = \epsilon_{HOMO} + \epsilon_{LUMO} + U$, respectively.

These probabilities obey the rate equation

$$\dot{\mathbf{P}} = \mathbf{W} \cdot \mathbf{P} \quad (3)$$

Where the elements of the rate matrix, $\mathbf{W}_{n,m} = W_{n\to m}$, describe the rate of transfer from state $|n\rangle$ to state $|m\rangle$. If this $n \to m$ transition is due to electron transfer from the electrodes (i.e. $|n\rangle$ has one electron less than $|m\rangle$) then $W_{n\to m}$ are defined as

$$W_{n\to m} = \sum_{\nu=L,R} \left[\left| \sum_{j=H,L} \gamma_\nu^j \langle n | d_j^\dagger | m \rangle \right|^2 \right] f_\nu(\Delta E_{nm}) , \quad (4)$$

where γ_ν^j is the rate for an electron to cross the molecule-electrode interface from the electrode $\nu = L, R$ into the state j (either the HOMO or the LUMO). γ_ν^j is proportional to the ν −electrode density of states. $\Delta E_{nm} = E_m - E_n$ is the difference in energy between the two molecular states.

The term in the parenthesis is simplified by the fact that the HOMO and LUMO are orthogonal states, leading to the expression for these rates if the $n \to m$ transition is due to electron transfer *from* the electrodes,

$$W_{n\to m} = \sum_{\nu=L,R} \gamma_\nu^m f_\nu (\Delta E_{nm}) \quad . \quad (5)$$

If the $n \to m$ transition is due to electron transfer *to* the electrodes, then the rates will be

$$W_{n\to m} = \sum_{\nu=L,R} \gamma_\nu^n (1 - f_\nu (\Delta E_{nm})). \quad (6)$$

The Fermi functions are $f_\nu(\epsilon) = \frac{1}{1+\exp\left(\frac{\epsilon-\mu_\nu}{k_B T}\right)}$, and the electrodes chemical potentials differ by the bias voltage, $\mu_{L,R} = \mu \mp V/2$.

The HOMO and LUMO states are coupled via the photon interaction, i.e. the system can absorb a photon and go from the HOMO to the LUMO and vice versa. If we denote the Fock states $|H\rangle$ and state $|L\rangle$ as molecular states with a single electron occupying the HOMO and LUMO respectively (with probabilities P_2, P_3), then the transition rate is given by (if the photon is at resonance with the HOMO-LUMO gap)

$$W_{|H\rangle\to|L\rangle} = \nu_{ph} \left|\langle L|a\, d_L^\dagger\, d_H|H\rangle\right|^2 , \tag{7}$$

where ν_{ph} is the net photon flux (number of photons absorbed by the molecule per unit time). Assuming that the molecular states are photon thermal states (assuming weak electron-photon coupling), the photon states are defined via $\langle a^\dagger a\rangle = n_B = \frac{1}{\exp\left(\frac{\omega_0}{kT}\right)-1}$, leading to the simple expression

$$W_{2\to3} = \nu_{ph}\, n_B, W_{3\to2} = \nu_{ph}\, (n_B + 1) \ , \tag{8}$$

and we set to $n_B = 1$ in the semi-classical limit. In fact, one can estimate n_B in these experiments. Consider the laser power of ~10 μW (as per the manufacturer specs, see below) from an optical fiber with a diameter of 600 microns, thus impinging a power of ~0.3×10^2 W/m^2 . If the molecular cross-section is ~$10^{-18} m^2$, this implies power absorption of ~10^2eV/s, corresponding to ~50 photons/s . This value is absorbed into ν, which is thus comprised of the power input, molecular cross section, fluorescence decay rate/exciton life-time etc, and is thus left as a fitting parameter.

We also point out that one can add to the model a term which corresponds to spontaneous absorption/emission. Such a term would have a similar form as in Eq. (8), but with the thermal Bose-Einstein distribution, which at the photon energy of the HOMO-LUMO gap, essentially vanishes. This results in an effective fluorescent decay term $W_{3\to2} = \nu_{FL}$. One can estimate the fluorescent time at $10^7 - 10^9 s^{-1}$, which results in no significant change to the results presented in the main text. [1, 2]

The steady-state solution $\mathbf{P}_{ss}$ in the presence of illumination and bias voltage (which is required to find the conductance) is found by solving $\dot{\mathbf{P}} = \mathbf{0}$, i.e. finding the kernel of the rate matrix $\mathbf{W}$. To find the current, one first notes that the total occupation of the molecule is $n = P_2 + P_3 + 2\, P_4$. The general expression for the current is then $I_{tot} = e\frac{d(P_2+P_3+2\,P_4)}{dt}$. Using Eq. 3 and substituting the steady-state solution, one finds that the total current can be written as $I_{tot} = I_L + I_R = 0$, where $I_{L,R}$ is the current flowing from the left electrode and to the right electrode, respectively, and are equal in magnitude and opposite in sign at the steady state, and one can set $I = I_L$. It is straightforward to show that setting $U = 0$ and without bias, the Eq. 16 of Ref. [Galperin & Nitzan 2005] is reproduced (at resonance). The conductance, which is the goal of this calculation, is defined as $G = \lim_{V\to0} \frac{dI}{dV}$.

We note here that this approach to steady-state conductance implies continuous wave illumination (as is done experimentally). Thus, while a description of the molecular system as "absorbing a photon and exciting an exciton" is tempting, the model itself assumes that this occurs continuously, thus affecting the conductance at the steady state. This implies that the transport histogram under illumination will only have one peak – as we observe experimentally - and not two peaks as seen in, e.g. Ref. 20 in the main text.

2. Ruling out junction asymmetry as the cause for photoconductivity

As pointed in the introduction in the main text, one possible source of photoconductivity is an asymmetry in the couplings to the HOMO and LUMO between the left and right electrodes. This seems not to be the case in our junctions, considering the fact that the PTCDI molecular junctions are symmetric. However, asymmetry may arise in the junctions due to random changes in the binding configurations between the molecule and the gold contacts. To evaluate the magnitude of the required asymmetry, we plot in Fig. S1 the ratio between the conductances under illumination and in the dark (i.e. the photoconductivity), as a function of the ratio between the couplings to the left and right electrodes, respectively. From Fig. S1 one can see that to reach photoconductivity ratio of ~1.5, as observed in the experiments, an asymmetry ratio of 10^3 is required *on average*. This is, of course, highly unlikely in a pre-defined symmetric molecular junction, thus ruling our junction asymmetry as a source of photoconductivity in our system.

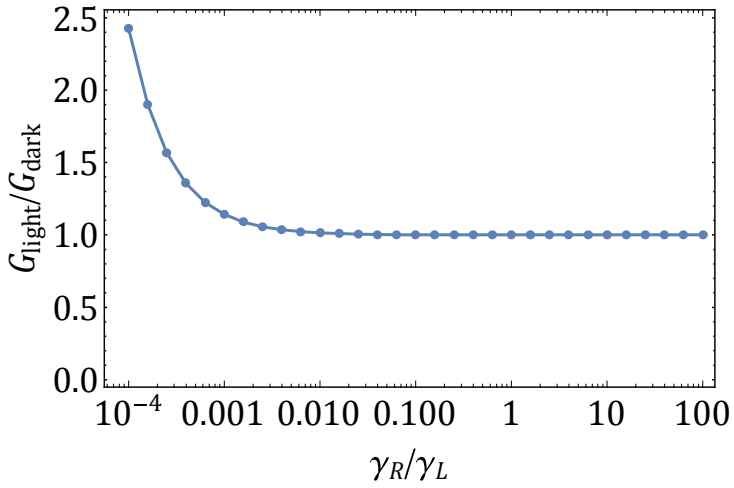

Figure S1: Photoconductivity as a function of the left-right coupling asymmetry. To reach a ratio of ~1.5 there shuld be an unlikely 3 orders of magnitude difference between the couplings.

3. Heating as a possible source of photoconductivity

Another source for photoconductivity might be heating. Naively, one would make the following argument: consider a molecular junction with some typical conductance. Now, if the system is heated, then the electrodes might expand due to thermal expansion. Then, the distance

between the electrodes is smaller and the conductance increases. For this argument, even a sub-nanometer change in volume might affect conductance to a measurable level.

Before we argue that this is not the case in the presented set of experiments, we estimate the possible change in temperature. To do this, we write a simple heat-balance equation,

$$C_v \frac{d}{dt} T = W_{in} - G(T - T_{amb}) \qquad (9)$$

where T is the sample temperature, C_v the gold electrode heat capacity, G the thermal conductivity (i.e. the rate at wich energy is dissipated to the ambient) and T_{amb} the ambient temperature. W_{in} is the power (per unit volume) absorbed by the gold electrode. For a laser power of ~9μW, Au thermal conductance of ~$5 \times 10^{14}\mathrm{W/Km^3}$, and an estimated electrode volume of V_{Au}~$10^{-12}m^3$, the steady state solution of Eq. (9) predicts a temperature rise of ~$10^{-3} - 10^{-4}\mathrm{K}$. This is well within the thermal noise of the system (noting that experiments are performed at room temperature). It is therefore unlikely that this effect will be observed in the conductance.

Furthermore, we argue that with the experimental protocol that we use, even more substantial heating would not show a different in the conductance histogram, and the reason is as follows. In the experiments, the junction is stretched until a single molecule junction is formed, where the conductance is collected. Then, the same stretching experiment is performed under illumination. So, even if heating took place which would make the junction smaller (due to thermal expansion), that would only reflect in the stretching curve of the conductance (e.g. inset to Fig. S4), but not in the value of the conductance, which would still correspond to that of the molecule.

4. Experimental details

1) **Synthesis of N,N' –di(1,4-diaminophenyl)-perylene-3,4,9,10- tetracarboxylic diimide (N-PTCDI)** as shown in Figure S2:

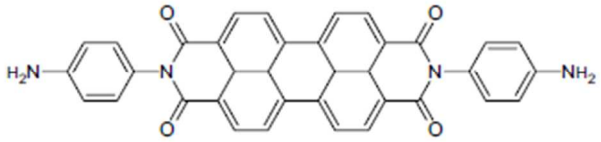

Figure S2: Molecule structure of N,N' –di(1,4-diaminophenyl)-perylene-3,4,9,10- tetracarboxylic diimide (N-PTCDI)

N-PTCDI used in the experiments was synthesized following the simple methods described by Schmidt, et.al. [3] Briefly, 1.03 g (2.63 mmol) perylene-3,4,9,10-tetracarboxylic dianhydride and 2.84 g(26.25 mmol) *p*-Phenylenediamine (Aldrich), were refluxed with a small amount of Zn(Ac)2·2H2O as catalyst in 50 mL m-cresol. After 12 h the mixture was cooled to room temperature, the solvent was removed, and the obtained N-PTCDI was purified by sublimation. N-PTCDI is slightly soluble in DMF, DMSO, and little less soluble in other solvents like

chloroform, toluene, and dioxane. The N-PTCDI molecules were therefore absorbed on two the god substrate from DMSO solution for the STM break junction measurements throughout all the measurements. For each measurement, the N-PTCDI sample solution was dropped on a freshly hydrogen flame annealed Au(111) surface for 10 min incubation followed a thorough washing with water and ethanol alternatively. After adding Toluene in the Teflon sample cell to prevent contamination, the conductance measurement was immediately performed.

2) UV-Vis absorption spectrum

UV–Vis absorption spectrum of N-PTCDI in Toluene solution was measured with a UV-Vis spectrophotometer (SHIMADZU UV-1700). Two discrete absorption peaks at ~498 nm and 552 nm were observed (Figure S3).

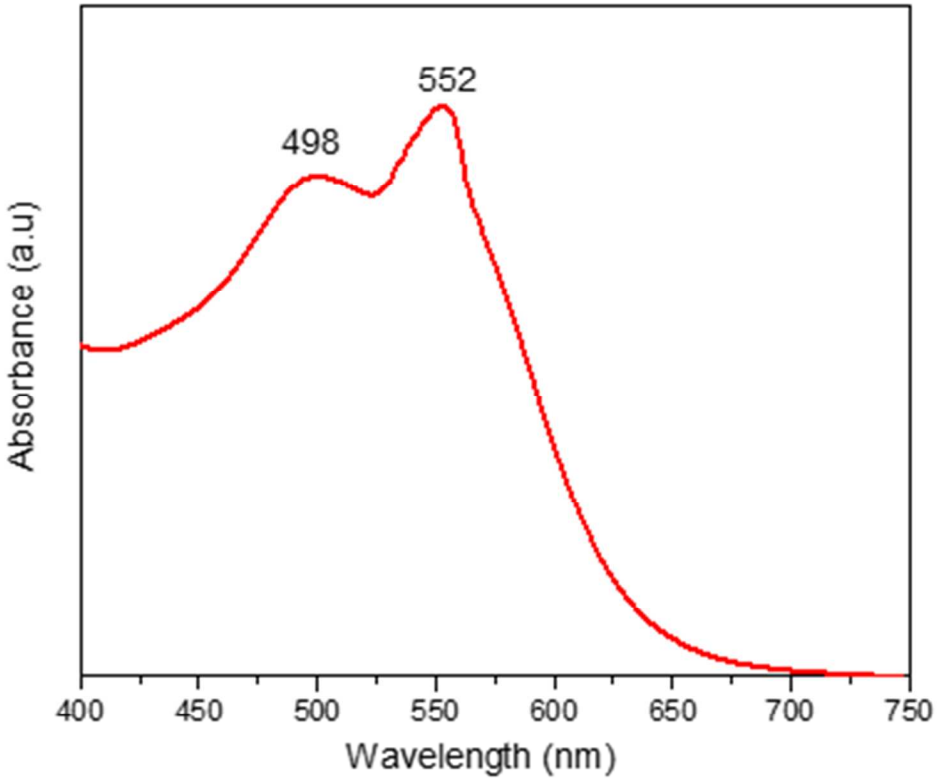

Figure S3: UV–Vis absorption spectrum of N-PTCDI in Toluene.

3) Conductance measurements

A single PTCDI molecule was wired to two gold electrodes to form a molecular junction using the STM break junction techniques developed in our lab at UGA. Briefly, the Au-N-PTCDI-Au molecular junctions were formed when STM tip approached the Au surface covered with a monolayer of N-PTCDI molecules and then broke when STM tip retracted away from the surface. During each of the tip retracting process, a conductance trace was recorded. By repeating this,

over 1000 conductance traces were collected for the construction of the final conductance histogram. The conductance measurement was carried out under a bias voltage of 0.3V at room temperature. The 0.3 bias is within the linear region of the IV curve (Figure S4).

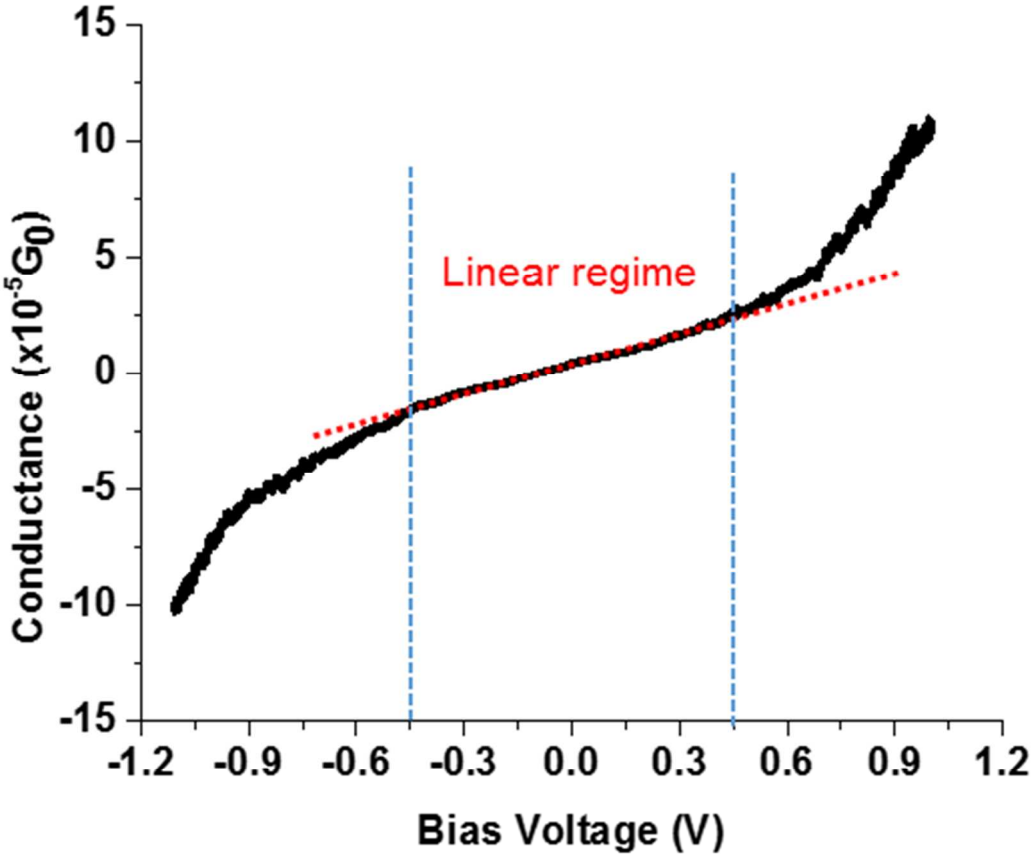

Figure S4: IV curve of Au-N-PTCDI-Au junction measured by sweep the bias voltage between -1.2V and +1.2V, the linear region is determined to range from -0.5V to +0.5V.

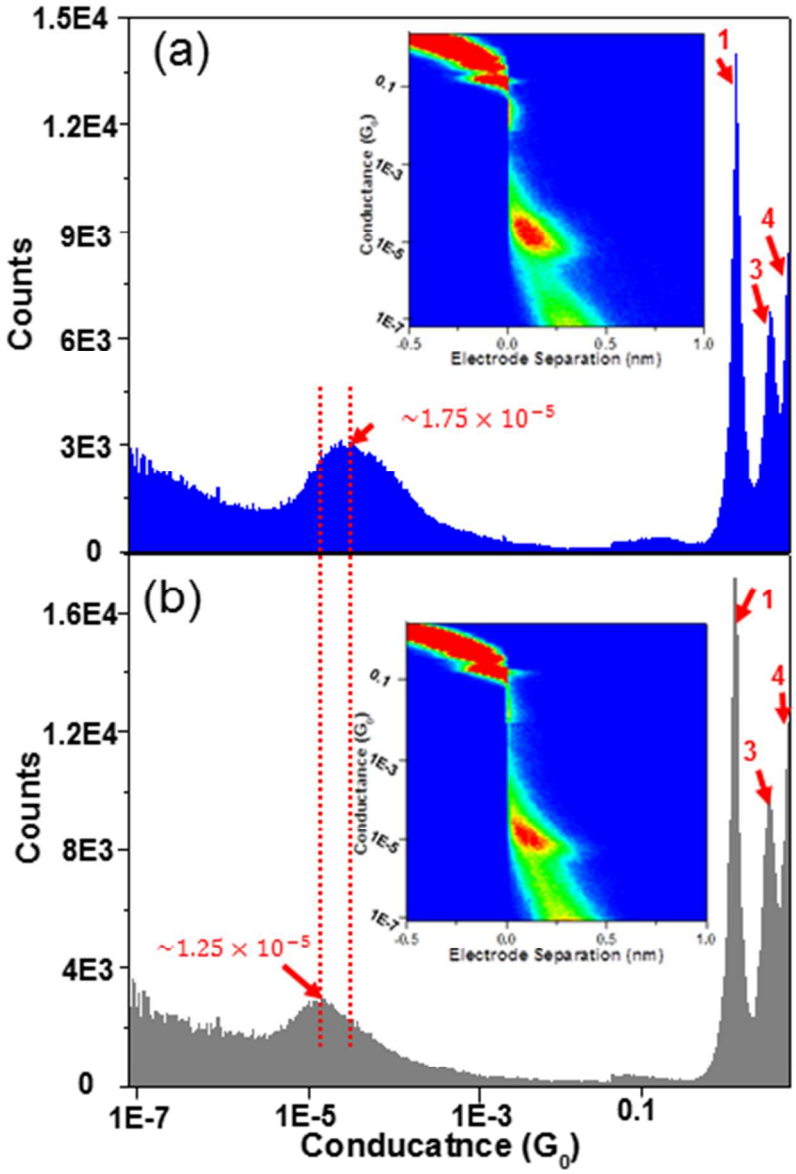

Figure S5: Log scale conductance histograms of Au-N-PTCDI-Au junction with (a) and without (b) photo emission constructed from over 1000 log-scale traces.

In order to make sure the good contact of STM tip with the Au substrate is fully established in each of the approach-retracting circle, a logarithmic-scale STM scanner was first applied CSM to monitor a broad range of conductance including the gold quantum contacts. This also offered a first glance at the possible conductance of Au-N-PTCDI-Au junction with and without applying the 495nm photon emissions. As is shown in Figure S5, sharp peaks at integer multiples of conductance quantum G_0 (~77μS) reveal the gold quantum contacts were well established in the histograms before (Figure S5 (b)) and after (Figure S5 (a)) the photoemission. The stretching distance of the junction in both cases are around 0.2nm (Inset of Figure S5) also shows that the Au-N-PTCDI-Au junction remains as stable after photo emission. In addition, the histogram also exhibited apparent peaks at lower conductance range: around $1.25\times10^{-5}G_0$ and $1.75\times10^{-3}G_0$,

respectively, strongly suggesting that under the photo emission, the conductance values of the N-PTCDI molecule is increased.

Log-scale data offered a complete scope of possible locations of conductance peaks, but failed to provide highest resolution of details which is necessary for electrical measurements at single-molecule level. In order to accurately determine the conductance value and gain more details of the N-PTCDI molecular junction, linear scale STM scanner was then used and the results were reported in the main body of the manuscript.

1. Huang, C., S. Barlow, and S.R. Marder, *Journal of Organic Chemistry,* 2011. **76**(8): p. 2386-2407.
2. Sadrai, M., et al., *Journal of Physical Chemistry*, 1992. **96**(20): p. 7988-7996.
3. Neuber, C., et al., *Journal of Materials Chemistry*, 2006. **16**(34): p. 3466-3477.